1996

Artificial Maturation of Alginite and Organic Groundmass Separated from Torbanites

Michael A. Kruge
Montclair State University, krugem@mail.montclair.edu

Patrick Landais
CNRS-CREGU

David F. Bensley
Southern Illinois University Carbondale

Preprint: Kruge M. A., Landais P. and Bensley D. F. (1996) Artificial maturation of alginite and organic groundmass separated from torbanites. *Organic Geochemistry* **24**:737-750.
https://www.sciencedirect.com/science/article/abs/pii/0146638096000642
https://doi.org/10.1016/0146-6380(96)00064-2

Artificial Maturation of Alginite and Organic Groundmass Separated from Torbanites

MICHAEL A. KRUGE[1,2], PATRICK LANDAIS[2] and DAVID BENSLEY[1,3]

[1]Dept. of Geology, Southern Illinois University, Carbondale, IL 62901-4324 (USA)
[2]CNRS-CREGU, BP 23, 54501 Vandœuvre-lès-Nancy cedex (France)
[3]Carbon Consultants International, Inc., PO Box 819, Carbondale, IL 62903 (USA)

Abstract— The two principal organic constituents — *Botryococcus*-related alginite and organic groundmass — were isolated by density separation from two torbanite samples (from the Stellarton Fm., Nova Scotia, Canada and the King Cannel, Utah, USA). The groundmass consisted of degraded algal, bacterial and terrestrial plant debris. Aliquots of alginite and groundmass were separately heated in gold tubes for 24 hr. with 70 MPa confining pressure, at fixed temperatures ranging between 250 and 375°C. The 250, 300 and 325°C experiments run on the alginite produced very low yields of $CHCl_3$-extractable organic matter (EOM), indicating that very little of the generation potential had been tapped. The alginite reached the onset of generation at 350° and peaked at 375°. The groundmass exhibited a distinctly different response to heating. Its 300, 325 and 350°C experiments showed a progressive increase in EOM yield with increasing temperature, producing more EOM than the corresponding alginite runs, in spite of the lower initial generation potential of the groundmass. However, EOM yields were lower at 375°C, indicating that its peak generation had occurred at 350°. After heating, the $CHCl_3$-extracted residues were analyzed by Rock Eval and flash pyrolysis-GC/MS to determine the remaining petroleum potential and monitor the alterations in the macromolecular structure. In nature, petroleum generated from a torbanite would be a mixture of the liquids generated by each of its components, in a blend that would change as thermal alteration progressed, as the various constituents each reached their peak of generation. Such a multi-component model of torbanite composition can serve to improve predictions of oil generation from torbanites and related source rocks in sedimentary basins.

Key words— alginite, *Botryococcus*, organic groundmass, torbanite, artificial maturation, confined pyrolysis, flash pyrolysis, density separation

Short title— Artificial maturation of macerals

INTRODUCTION

Torbanites are organic-rich, non-marine deposits with a prominent algal component. This alginite is typically derived from a colonial alga similar to the extant *Botryococcus braunii* , undergoing selective preservation of the thick outer cell walls, which are composed of a degradation-resistant, aliphatic biopolymer (Largeau et al., 1984; Derenne et al., 1988a; 1988b). Many torbanites also have significant quantities of fine-grained organic matrix or groundmass (Combaz, 1980). The groundmass may include algal, bacterial, vitrinitic and inertinitic debris, often partly biodegraded or partly oxidized at the time of deposition. Algal material within the groundmass may contain non-resistant *Botryococcus* components, such as cell constituents, polysaccharide inner cell walls or lipids from the outer walls (Landais et al., 1993) or it may derive from other, less massive types of algae. The degree of chemical similarity between the alginite and the groundmass of a particular torbanite is a function of the magnitude of the algal contribution to, and the homogeneity of the groundmass, as well as the extent of bacterial degradation.

As the heterogeneous, polymeric nature of most sedimentary organic matter greatly complicates its chemical analysis, any successful subdivision into components or groups of components may aid in elucidation of chemical structures. While in-situ analytical techniques, such as micro-FTIR (Landais et al., 1993) and laser micropyrolysis (Stout, 1993), offer some advantages, physical separation by density still provides the best method for preparing milligram to gram quantities of reasonably pure macerals for chemical analysis and experimentation. Coal maceral concentrates separated by DGC (Crelling, 1989) have become available in recent years and have been the subject of several studies (e.g., Nip et al., 1988; 1992; Landais et al., 1991; Kruge et al., 1991; Blanc et al., 1991). Previous work on kerogen DGC fractions has been more limited (Senftle et al., 1988; Kruge et al., 1989) until recently, when kerogen macerals from petroleum source rocks and sapropelic coals began to be investigated in detail (Stankiewicz et al., 1994a; 1994b; Stankiewicz, 1995; Han et al., 1995; Han, 1995).

Artificial maturation studies have traditionally used whole kerogen, coal or source rock as starting materials for heating experiments (e.g., Lewan, 1985; Saxby et al., 1986; Landais et al., 1989a). Yet it has long been recognized that kerogen and coal are complex, heterogeneous substances, in most cases being mixtures of macerals of diverse biologic origin. Furthermore, the response to geothermal heating of a kerogen or coal is a function of the combined thermal responses of its individual components. To better understand the petroleum generation process, it is desirable to study the behavior of the individual macerals separately. Artificial coalification studies of the macerals isolated from humic coal documented their distinctly different responses to thermal stress (Landais et al., 1989b; 1991; Kruge and Landais, 1992).

The chief variables in closed pyrolysis experiments used for laboratory simulation of organic maturation include temperature, duration of heating, the use of isolated kerogen *vs.* a kerogen/mineral mixture (natural or artificial), hydrous *vs.*

anhydrous conditions, and the use of metal *vs.* glass reactors (e. g., Lewan, 1985; Comet et al., 1986; Saxby et al., 1986; Tannenbaum et al., 1986; Landais et al., 1994; Michels and Landais, 1994; Michels et al., 1995). The role of confinement is paramount, so that the effluents can reach pressures of at least several MPa, permitting deactivation by recombination of hydrogen radicals (Monthioux et al., 1985; 1986; Landais et al., 1994; Michels et al., 1995).

This study differed from most other artificial maturation work in that the variable of organic matter type was isolated as completely as possible. Two organic-rich rocks were chosen based on two criteria — 1) there were two dominant and chemically distinctive organic components in each, in both cases alginite and organic groundmass and 2) the samples were of low thermal maturity, so that sufficient natural generation potential remained to make the experiments worthwhile. For each rock sample, we were assured that both organic components had experienced exactly the same depositional and diagenetic history. The objectives were 1) to document the chemical differences in the alginite and organic groundmass and relate them to their different biological precursors and 2) to test the hypothesis that the diverse organic components of the torbanites should respond differently to the same thermal stimulation.

EXPERIMENTAL

Samples

The first sample was a torbanite from the Coal Brook Member of the Upper Carboniferous Stellarton Formation, collected at Shaw Pit, New Glasgow, Pictou county, Nova Scotia, Canada. Aspects of the geology and geochemistry of the organic-rich rocks of this formation have been presented by Macauley and Ball (1984), Hutton (1986), Naylor and Smith (1986), Kalkreuth and Macauley (1987), Püttman and Kalkreuth (1989), Kalkreuth et al. (1990), Smith et al. (1991) and Yawanarajah and Kruge (1994). The organic fraction of this sample was determined by petrographic examination to be composed primarily of yellow-orange fluorescing alginite (*Botryococcus*) and a fine-grained component (groundmass), which under white light appeared vitrinitic, but under blue light had a dull yellow-brown fluorescence. The groundmass consisted of a fine disseminated matrix of vitrinitic/alginitic constituents with a minor inertinite component. In addition to the *Botryococcus* alginite, there was also laminar alginite, measuring between 10 to 50 μm in length. Vitrinite reflectance was low (≈0.55% Ro), but evidently strongly suppressed. Alginite fluorescence intensities were weak, indicating that the sample had already entered the oil window, confirmed by the distribution pattern of hopanes in the extract of the raw sample.

The second sample was a torbanite from the Cenomanian-Turonian King Cannel seam, Kane county, Utah, USA, described in detail by Given and others (1985). The organic component of this sample was dominated by vitrinitic and inertinitic macerals with large *Botryococcus* alginite. The term "cannel" is a

misnomer in this case, as alginite rather than sporinite was the predominant liptinite maceral. The weakly-fluorescing groundmass was highly heterogeneous, with generally distinct boundaries noted between maceral groups. Low vitrinite reflectance and high fluorescence intensity indicated that the sample had not yet reached the oil window, confirmed by the presence of hopenes and $\beta\beta$ hopanes in the extract of the raw rock. There was only minor peripheral diffusion of fluorescing material into the vitrinite matrix observed adjacent to alginite macerals. Amorphinitic material (probably of algal origin) was dispersed throughout the groundmass.

Maceral separation

Concentrates of the alginite and groundmass from both samples were prepared from CH_2Cl_2-extracted, demineralized kerogen by density separation using methods described previously (Bensley and Crelling, 1994; Stankiewicz et al., 1994b; Han et al., 1995). In brief, 2 kg of each sample were crushed to 75 μm size and extracted with excess CH_2Cl_2 in a sonicator, repeating with fresh solvent until clear. Extraction residues were demineralized using 20% HCl followed by 48% HF. The residues after acid treatment were centrifuged in an aqueous CsCl solution with a density of 1.6 g/mL to separate pyrite and remaining silicates from the organic matter (OM). After the samples were washed and dried, they were treated with liquid nitrogen to induce fracturing in the ductile liptinitic macerals, which allows for easier breakage during micronization (Stankiewicz et al., 1994b). OM concentrates thus prepared were reduced to micron size in a Garlock FMT mill at 20°C in a nitrogen atmosphere (Stankiewicz et al., 1994b). The concentrates were extracted again with CH_2Cl_2.

Aliquots (2 g) of the extracted, micronized residues were suspended in water by means of an ultrasonicator and layered on the top of a CsCl density gradient (1.00-1.60 g/mL), following published methodology (Dyrkacz et al., 1981; 1984; 1991; Dyrkacz and Horwitz, 1982; Crelling, 1988; 1989; Bensley and Crelling, 1994; Stankiewicz et al. , 1994b; Han et al., 1995). Petrographic pellets of the fractions were examined and it was determined that high purity (>95 vol. %) alginite was found in density fractions in the 1.00-1.10 g/mL range for the Stellarton sample and at 1.00-1.11 g/mL for the King Cannel (Fig. 1). In both cases, the groundmass and alginite components produced distinct peaks on the DGC profile, resembling the profile of an Australian torbanite previously reported (Han et al., 1995). Groundmass of the same purity was found in the 1.16-1.22 g/mL range (Stellarton) and at 1.20-1.25 g/mL (King). Using the above density ranges as cut points, the remaining Stellarton and King OM concentrates were centrifuged sequentially in several CsCl solutions of single densities to isolate the alginite and groundmass, yielding several grams of each fraction. The four end products were again extracted with CH_2Cl_2 and examined petrographically for purity confirmation. Although the OM particles were reduced to the 10 μm size range during processing, diagnostic petrographic features (fluorescence color and intensity under blue light and reflectivity under white light)

were still recognizable. A similarly successful density separation of a torbanite's organic constituents has been reported in detail (Han et al., 1995).

Confined pyrolysis in gold tubes

Aliquots (75-160 mg) of the alginite and groundmass from the two samples were separately heated under argon in sealed gold tubes for 24 h at 70 MPa pressure at temperatures ranging from 250 to 375°C (Table 1). The autoclaves and methods used for confined pyrolysis have been described previously (Monthioux et al., 1985; Landais et al., 1989a). After 24 hr, the tubes were quenched and removed from the autoclaves. They were pierced and gas contents determined by weight loss, after degassing overnight at 40°C. The tubes and their contents were extracted with $CHCl_3$ for 45 min. under reflux. The extracts were concentrated by rotary evaporation and deasphaltened with *n*-heptane. Saturated and aromatic hydrocarbons were separated from the deasphaltened extract by liquid chromatography (LC), eluting with CH_2Cl_2 on an alumina microcolumn. The polar fraction was eluted with CH_3OH. The saturates and aromatics were separated on a silica microcolumn, eluting with *n*-pentane and 2:1 *n*-pentane/CH_2Cl_2 respectively. Several samples had very low yields of extractable material (EOM $\leq$ 25 mg/g, Table 1). These extracts were subjected to LC without deasphaltening, to minimize losses during manipulation.

Gas chromatography/mass spectrometry

Analysis of the saturate and aromatic fractions were performed using an HP 5890 Series II gas chromatograph with an HP 5972 Mass Selective Detector and a 60 m DB-5MS column (0.25 mm i.d., film thickness 0.1 μm). The column oven was operated under the following program: 40-130°C at 15 °/min., 130-300° at 3°/min. and then isothermal for 12 min. The on-column injector was temperature programmed to remain 3°C above the oven temperature. The MS was operated in Selected Ion Mode at 1.1 scans/sec for saturates and 0.9 scans/sec. for aromatics.

Flash pyrolysis of the extracted residues from the gold tubes was performed using an SGE Pyrojector II, coupled to the same GC/MS system described above, except that standard split injection was employed. The temperature program was isothermal for 5 min. at 40°C, then ramped 5°C/min. to 300°C and isothermally held for 15 min. The mass spectrometer was in full scan mode (50-550 daltons, 0.9 scans/sec., 70 eV ionization voltage). The Pyrojector furnace was held at a constant temperature of 620°C, with He carrier gas pressure maintained 30 kPa above that of the GC injector. Between 0.2 and 0.8 mg of sample were introduced into the furnace with a syringe designed for use with solids. Flash pyrolysis-GC/MS peaks were identified based on mass spectra and GC retention indices, with reference to the Wiley computerized mass spectral library and the literature (Radke et al., 1990; Hartgers et al., 1992; Nip et al., 1992; Sinninghe Damsté et al., 1992; 1993; Kruge and Bensley, 1994).

Figure 1. a) Density gradient centrifugation (DGC) results for the Stellarton organic matter. Alginite and groundmass density ranges are shown. b) DGC profile for the King Cannel organic matter.

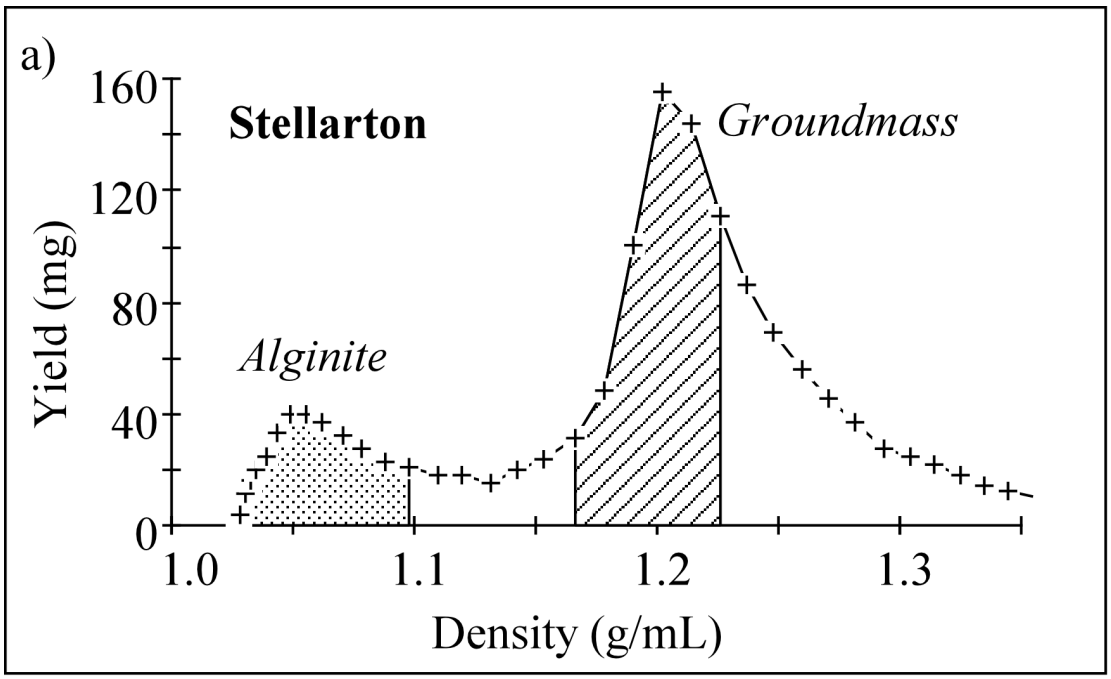

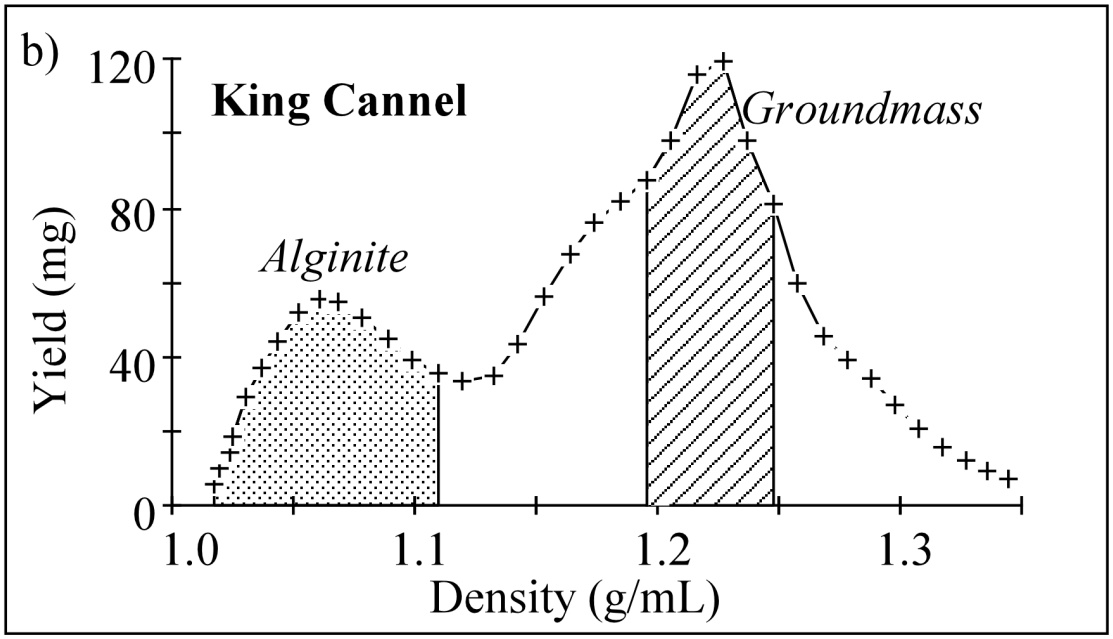

Table 1. Samples and bulk geochemical data from confined pyrolysis experiments. Initial OM: amount of organic matter used for pyrolysis. EOM: extractable organic matter formed during pyrolysis. TOC: total organic carbon determined by the Rock Eval apparatus. S2: amount of pyrolyzable organic matter (Rock Eval). HI: Rock Eval hydrogen index. All Rock Eval data collected on solvent-extracted residues or unheated samples.

Sample	Temperature (°C)	Gas/ Initial OM (mg/g)	EOM/ Initial OM (mg/g)	Residue/ Initial OM (mg/g)	Satuates/ Initial OM (mg/g)	Aromatics/ Initial OM (mg/g)	Polars/ Initial OM (mg/g)	TOC (%)	S2 (mg/g)	HI (mg S2/ g TOC)
Stellarton Fm.										
Alginite	unheated							70.2	565	805
Alginite	250	8	6	960	2	3	1	73.7	603	818
Alginite	300	7	12	927	2	3	8	75.6	633	838
Alginite	325	9	28	956	16	5	3	77.7	621	800
Alginite	350	11	180	776	35	35	87	79.9	597	747
Alginite	375	45	640	208	172	115	214	73.4	91	124
Groundmass	unheated							79.9	348	435
Groundmass	250	21	15	957	3	5	8	78.1	335	428
Groundmass	300	9	70	900	6	17	35	83.3	334	401
Groundmass	325	20	135	817	12	13	81	83.6	293	351
Groundmass	350	46	260	629	30	33	117	74.4	123	165
Groundmass	375	90	187	624	59	45	74	69.9	37	53
King Cannel										
Alginite	unheated							69.0	624	906
Alginite	250	5	63	930	3	2	51	70.8	642	906
Alginite	300	15	25	915	4	6	16	72.5	633	873
Alginite	325	16	67	872	11	12	36	75.4	637	846
Alginite	350	34	336	596	48	62	177	75.1	550	733
Alginite	375	94	558	208	181	178	152	70.6	51	72
Groundmass	unheated							82.2	375	457
Groundmass	250	5	9	965	0	2	7	80.9	315	390
Groundmass	300	13	57	881	6	10	30	83.4	276	331
Groundmass	325	31	136	804	13	17	78	75.2	190	253
Groundmass	350	52	246	636	34	35	122	74.8	96	129

RESULTS AND DISCUSSION

Confined pyrolysis yields

The bulk yields of the confined pyrolysis experiments were determined by monitoring two parameters — gas production and solvent-extractable organic matter (EOM), both in proportion to the initial quantity of OM pyrolyzed (Table 1). Gases likely included methane and other light hydrocarbons, as well as CO, CO_2, H_20 and H_2S, although the gas contents were not analyzed. The Stellarton alginite produced little gas (≤11 mg per g initial OM) during the four lower temperature experiments (250-350°C). At 375°, gas production rose to 45 mg/g. The Stellarton groundmass was consistently more gas prone, yielding 20 mg/g gas at 325°, 46 mg/g at 350° and 90 mg/g at 375°C. It is noteworthy that the increase in gas production with increasing temperature was more gradual for the groundmass than for the alginite. The King Cannel alginite produced between 5 and 16 mg/g gas in the 250, 300 and 325° experiments, increasing to 34 mg/g at 350°, then to 94 mg/g at 375°C. As in the case of the Stellarton, the King groundmass was more gas-prone than its companion alginite, yielding 31 mg/g gas at 325°, increasing to 52 mg/g at 350°C. A 375° experiment was not performed for the King groundmass.

The EOM yields of the Stellarton alginite were very low at lower temperatures, increasing from 6 to only 28 mg per g of initial OM from 250-325°C (Table 1, Fig. 2). At 350°, the yield rose to 180 mg/g, while at 375°, EOM jumped to 640 mg/g, indicating that the material was at or near peak oil generating conditions. The Stellarton groundmass behaved very differently, with EOM yields increasing gradually from 15 to 260 mg/g over the 250-350°C range, surpassing the yields of the alginite at every temperature step (Fig. 2). However, at 375° the groundmass produced less EOM (187 mg/g), thus peak liquid generation conditions for the groundmass were at or near 350°C, significantly lower than its companion alginite. Like the Stellarton, the King alginite produced little EOM (<70 mg per g initial OM) during the 250, 300 and 325°C experiments (Table 1, Fig. 2). The King alginite produced slightly more than the Stellarton, reflecting its lower initial thermal maturity, having not already undergone any significant natural oil generation. Production increased sharply to 336 mg/g at 350° and rose further to 558 mg/g at 375°C. Its companion groundmass demonstrated a gradual increase in EOM yields over the 250-350°C range, much like the Stellarton groundmass. In most lower temperature experiments, the Stellarton and King groundmass fractions actually produced proportionally more EOM than the corresponding alginites, even though Rock Eval hydrogen indices of the unheated fractions indicated that the alginites were about twice as oil-prone as the groundmass (Table 1). Alginites only produced EOM at or near their full generation potential at the highest temperature employed (375°C).

Figure 2. Extractable organic matter yields as a function of confined pyrolysis temperature for the Stellarton and King Cannel density fractions.

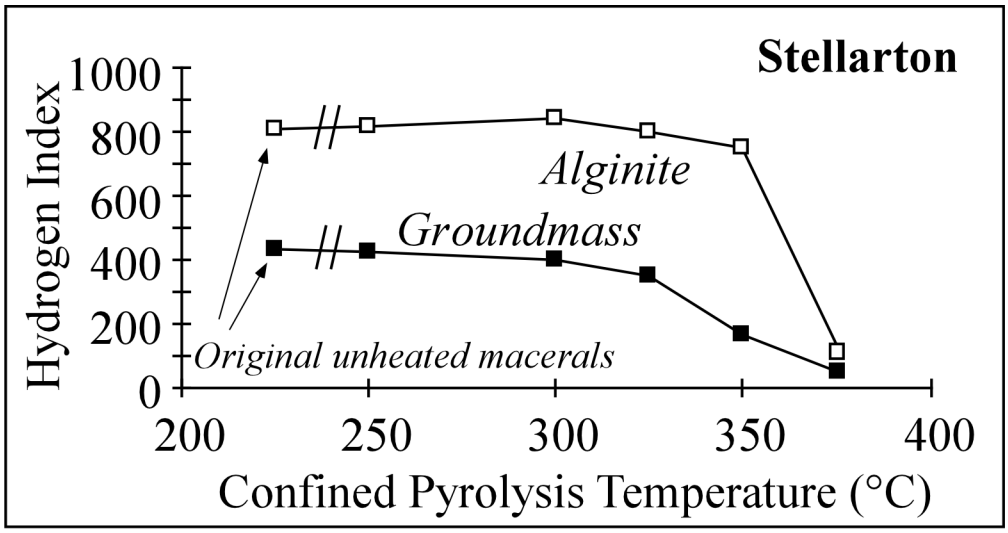

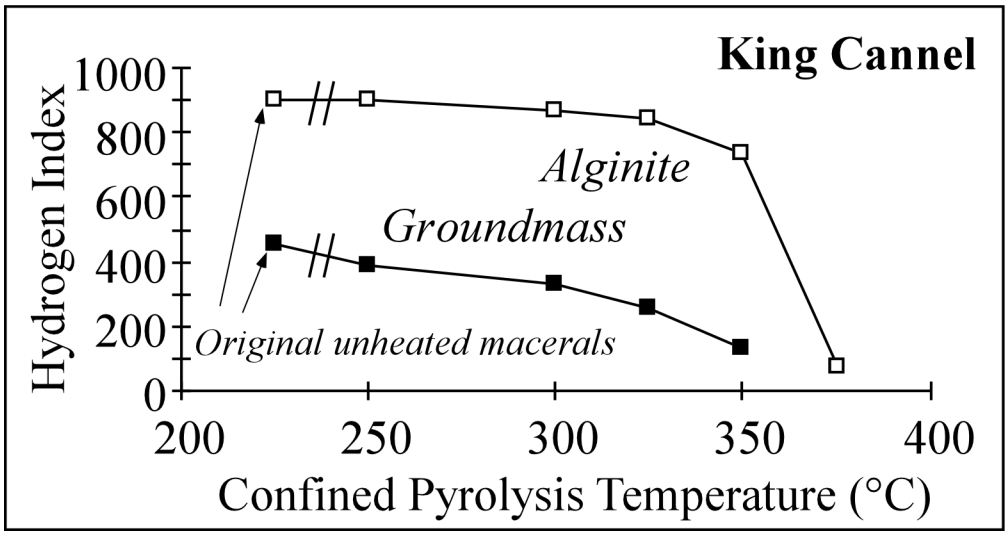

The amounts of the various LC fractions separated from the EOM also provided an interesting means of monitoring the progress of thermal alteration, especially when reported as a fraction of the initial organic matter heated (Table 1). The Stellarton alginite showed increasing production of saturates, aromatics and polars with increasing temperature, starting at a few mg/g at 250°C and rising sharply at 375°, at which temperature it produced between 115 and 214 mg/g of each LC fraction. The polars were the dominant fraction at 350°, comprising 55% of the deasphaltened extract and dropped to 43% at 375°, as the saturates rose in importance. The LC fractions from the Stellarton groundmass experiments presented a rather different picture. The polar compounds in particular showed a steady rise in yield from 8 to 117 mg/g between 250 and 350°, dropping to 74 mg/g at 375°. The groundmass produced saturates and aromatics in about the same quantities as the alginite over the 250-350° temperature range, with slightly more aromatics at low temperature. However, production at 375° was less than half that of the alginite. The EOM maximum observed for the groundmass at 350° was attributable to the high yield of polar compounds.

The production of saturate and aromatic hydrocarbons from the King alginite followed an evolutionary pathway similar to the Stellarton alginite, with a sharp rise in yields to about 180 mg/g at 375° (Table 1). The extracts from the highest temperature King alginite experiments were enriched in aromatics relative to those from the Stellarton. The polar compounds, however, reached a maximum yield of 177 mg/g at 350°, with only a slight decline at 375°, demonstrating the lower temperature generation of polar compounds. This "early" generation phenomenon was less clear for the Stellarton alginite, likely because of its higher initial maturity. The yields of the LC fractions for the King groundmass were similar to those of the Stellarton groundmass over the 250-350° range. They were higher than those of the King alginite at 300 and 325°, but were surpassed at 350°. Several deviations from trends are noted in low temperature samples, such as for the polar fractions of the 300° Stellarton and King alginite experiments, the gas yields of the Stellarton groundmass heated at 300° and the EOM of the 300° King alginite run (Table 1). These likely arise due to measurement uncertainties encountered with these small, low yield samples.

Confined pyrolysis residues

Since the density fractions were nearly mineral-free, monitoring the amount of solid residue after heating provided an additional means to observe the progress of thermal alteration. Residue ($CHCl_3$-extracted) accounted for 927-960 mg per g of initial OM of Stellarton alginite at 250, 300 and 325°C, indicating that very little of the material had been consumed (Table 1). At 350°, residue amounted to 776 mg/g, demonstrating that conversion had begun. Only 208 mg/g residue remained after heating at 375°, indicating that the great majority of the alginite had been converted to gases and liquids. The sharp decrease in residue at this temperature step matched the correspondingly abrupt increase in EOM and gases. The Stellarton groundmass

residues decreased gradually from 957 to 629 mg per g of initial OM from 250-350°C. By 375° the residue contents showed no further decrease, indicating a post-peak generation level of thermal alteration. Like the Stellarton alginite, the King alginite also showed little change over the 250-325°C range, producing 872-930 mg/g solid residue. At 350° residue had dropped to 596 mg/g and by 375°, there was only 208 mg/g residue, comparable to the Stellarton alginite (Table 1). The King groundmass residue, like that of the Stellarton, decreased smoothly with temperature increase, dropping from 965 to 636 mg/g over the 250-350°C temperature range.

Rock Eval. The Rock Eval hydrogen index (HI) is defined as the ratio of pyrolyzable OM to total organic carbon contents. It provided one of the most useful bulk parameters for observing the differences in thermal alteration pathways taken by the samples, measuring the remaining generation potential of raw, unheated samples as well as of extracted residues after heating. The HI for the unheated Stellarton organic concentrates were 805 (alginite) and 435 mg/g TOC (groundmass), indicating that the alginite had twice the oil generation potential of the organic groundmass, although both were oil-prone. There was no significant change in HI for the alginite after heating at 250, 300 and 325° (Table 1, Fig. 3), demonstrating that the experimental conditions were insufficiently severe to tap its generation potential. At 350°, the HI was reduced slightly to 747 mg/g, corresponding to the onset of generation, while by 375° the HI dropped precipitously to 124 mg/g, showing that the generation potential had been nearly exhausted. Although starting from a lower level of generation potential, the Stellarton groundmass began to significantly decompose at lower temperatures than did the alginite. Its HI dropped gradually from 428 to 53 mg/g over the 250-375°C range. The HI for both the alginite and groundmass varied inversely with the amount of EOM and volatiles produced.

The King alginite had an initially higher generation potential (HI = 906 mg/g) than the Stellarton alginite, but it also showed very little loss of that potential until 350°, at which point HI was reduced to 733 mg/g (Table 1, Fig. 3). Like the Stellarton, the King alginite displayed a severe loss of potential at the highest temperature, as heating at 375° left it with an HI of only 72 mg/g. The King groundmass, starting at an HI of 457, lost generation potential in a gradual, step-wise fashion, such that by 350° HI was reduced to 129 mg/g, following a pattern like that observed for the Stellarton groundmass.

Flash pyrolysis. Like the Rock Eval hydrogen index, flash pyrolysis (Py-GC/MS) permitted the characterization of the starting materials and the extracted residues from the heating experiments. The advantage of Py-GC/MS is its ability to provide details of composition on the molecular level using milligram-size samples. While both the unheated Stellarton alginite and groundmass were strongly aliphatic, the alginite had a significantly greater proportion of short-chain (C_8-C_{18}) *n*-alkanes and especially *n*-alk-1-enes. The groundmass displayed a greater predominance of aromatic and phenolic compounds. The same distinctions applied to the unheated King macerals, although its alginite yielded more aromatic products than the Stellarton. For both the King and Stellarton samples, the most important aromatic

hydrocarbons were the C_1 to C_4-alkylbenzenes, naphthalene and C_1 to C_3-alkylnaphthalenes. Phenanthrene, anthracene and their alkylated derivatives were also detected, but not in significant quantities. Thiophenes were detectable, but in low concentrations, as expected in these lacustrine samples. Since the Py-GC/MS results demonstrated that the unheated Stellarton and King samples were similar, the bulk results presented above revealed similar behavior and the Stellarton data set was more complete, the following discussion of the details of the Py-GC/MS results will be limited largely to the Stellarton alginite and groundmass.

The overwhelming predominance of aliphatic hydrocarbons is clearly evident in the total ion current (TIC) trace for the flash pyrolyzates of the extracted 250°C residue of the Stellarton alginite (Fig. 4). (It is important to remember that the temperatures cited throughout this discussion refer to the conditions of the day-long confined heating in gold tubes, not the flash pyrolysis temperature which was invariably 620°C.) The only significant non-aliphatic component was toluene. Three homologous series of normal hydrocarbons were detected — *n*-alkanes, *n*-alk-1-enes and *n*-a,w-alkadienes, as exemplified by the C_{11} members of these series (Fig. 4). These features were previously identified as characteristic of *Botryococcus*-related alginite and of Type I kerogens in general (Derenne et al., 1988b; Han et al., 1995). The alkenes were the major constituents, particularly over the C_7-C_{24} range. The 250° residue of the groundmass, while still highly aliphatic overall, had significantly more aromatic and phenolic compounds than did the corresponding alginite residue (Fig. 4). Among the normal hydrocarbons, the alkanes were more important, but the alkenes still dominated. The alkadienes were present, but were relatively weaker. C_{27} and C_{29} hopanes and hopenes were detected as minor components. Hopanoids have been previously recognized in flash pyrolyzates (Sinninghe Damsté et al., 1992), in particular from torbanite groundmass (Han et al., 1995), for which they provided direct evidence of a bacterial contribution. The flash pyrolyzates of the 250° extracted residues resembled those of the unheated macerals, indicating that little alteration had occurred at this low temperature, in accord with the Rock Eval and other data.

The flash pyrolyzates from the 300, 325 and 350° alginite experiments revealed no significant changes in composition as a function of increased temperature. There were some minor variations in normal hydrocarbon distributions and a slight decrease in aromaticity. By 350°, the *n*-alkane/*n*-alkene ratio had increased slightly over that at 250° (Figs. 4, 5). In contrast, the groundmass displayed continuous transformation as temperatures were increased, including relative decreases in concentrations of phenols, longer-chain (C_{19}-C_{29}) *n*-alkanes and the hopanoids. Comparison of the 350° groundmass residue with the 250° clearly illustrates these phenomena (Figs. 4, 5). The peak in production of polar compounds seen for the Stellarton groundmass EOM at 350° (Table 1) is likely due at least in part to the production of phenols, causing a corresponding depletion of phenolic structures in the residue. The 350° alginite residue continued to appear markedly more aliphatic than the groundmass heated at the same temperature (Fig. 5).

The residual material after heating alginite at 375° displayed major signs of thermal alteration (Fig. 6). There was a pronounced shift to shorter chain normal hydrocarbons and the *n*-alkenes were relatively much less important than at the 350° step. Alkadiene concentrations dropped to nearly negligible values. There was, however, no increase in aromaticity and the sample still appeared oil-prone. By 375°, the groundmass had undergone severe transformation, with only a few short-chain *n*-alkanes (C_{10}-C_{14}) predominating (Fig. 6). The relative contribution of phenols had declined, while the increase in naphthalenes contributed to a higher aromaticity, an indication of greater polycondensation. Its flash pyrolyzate thus contrasted sharply with that of the 375° alginite residue.

The greater reactivity of the groundmass at lower temperatures observed in the flash pyrolysis data was consistent with the image presented by the bulk analyses discussed above, such as the EOM yields, the amounts of residue and the hydrogen indices of the residues (Table 1, Figs. 2 and 3). Again, in accord with the bulk data, the Py-GC/MS results demonstrated that the alginite stubbornly resisted thermal decomposition until the highest temperature (375°) step.

Maturity ratios employing the relative quantities of various temperature-sensitive polyaromatic hydrocarbons have been applied occasionally to flash pyrolyzates (Requejo et al., 1992; Kruge and Bensley, 1994). Various ratios previously found to adequately track to thermal evolution of the vitrinite maceral used methylphenanthrenes and methylanthracenes (Kruge and Bensley, 1994). These parameters did not clearly document maturation trends in this case, perhaps due to the overall low maturity levels, although relative concentrations of anthracene and methylanthracenes were consistently observed to diminish at the highest temperature employed (375°C). One maturity parameter was of particular interest. It used several trimethylnaphthalene isomers quantitated using the Py-GC/MS data (Fig. 7) and was developed in light of previous empirical and theoretical work (Alexander et al., 1985; Budzinski et al., 1993; Kruge and Bensley, 1994). It demonstrated the ability to track the extent of thermal alteration, displaying for the most part an inverse relationship with the hydrogen index (Fig. 7). Values of this trimethylnaphthalene ratio (TMN) for the King and Stellarton alginites exhibited little change while HI remained high. The Stellarton values were greater, reflecting the fact that the sample was initially more mature. However by 375°, at which point the HI had dropped abruptly for both samples, the TMN also increased, particularly for the King alginite. Compared to their companion alginites, the groundmass fractions tended to have higher TMN values after the same amount of thermal stimulation, which appeared to be related to their lower potential to generate (lower HI). The TMN parameter, as applied to flash pyrolyzates, apparently responded to the progress of the oil generation reaction, rather than to absolute temperature, rising to its highest values as peak liquid generation levels were attained and surpassed.

Figure 3. Rock Eval hydrogen indices as a function of confined pyrolysis temperature for the Stellarton and King Cannel density fractions.

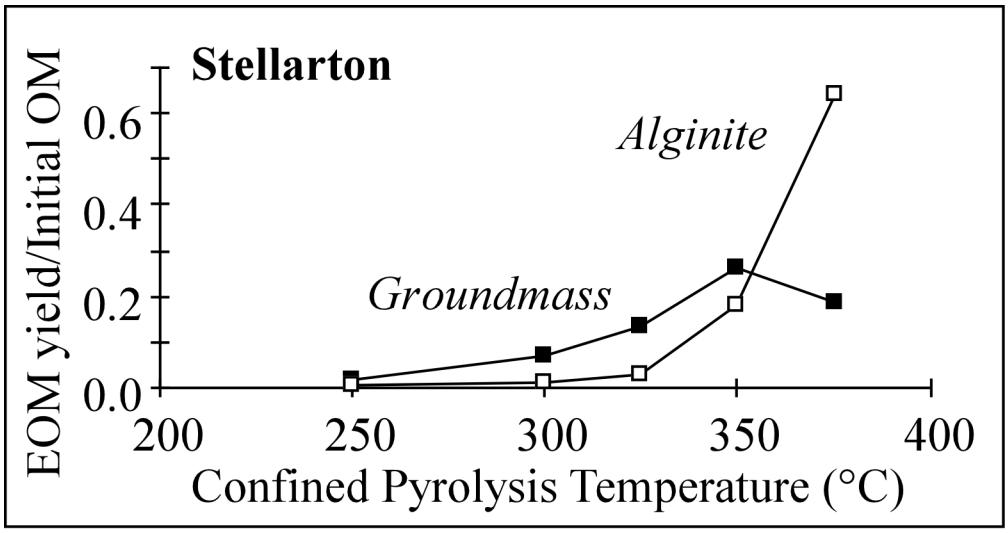

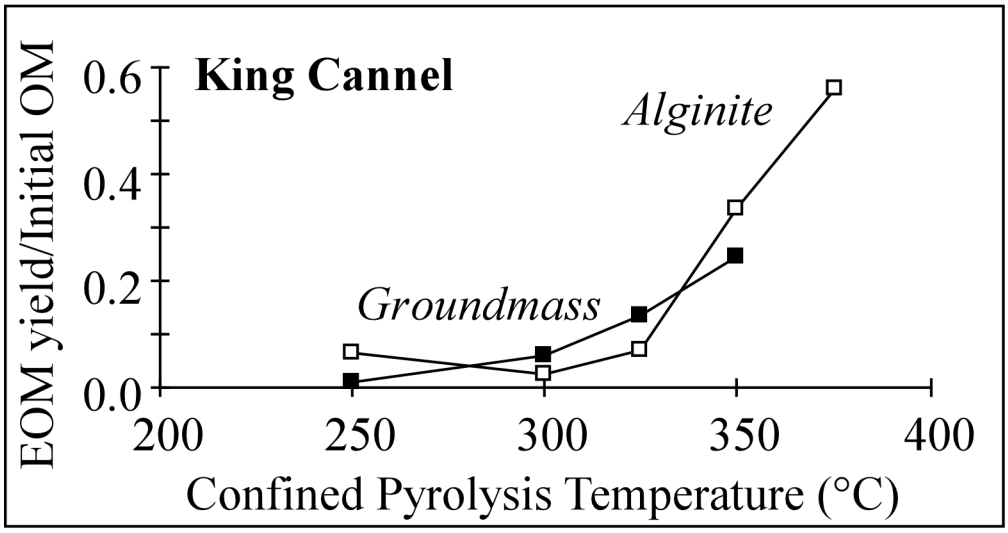

Figure 4. Total ion current traces of the flash pyrolyzates (620°C) of the solvent-extracted residues after heating Stellarton organic groundmass and alginite at 250°C and 70 MPa for 24 hr. Insets provide details of the *n*-C_{11} region.

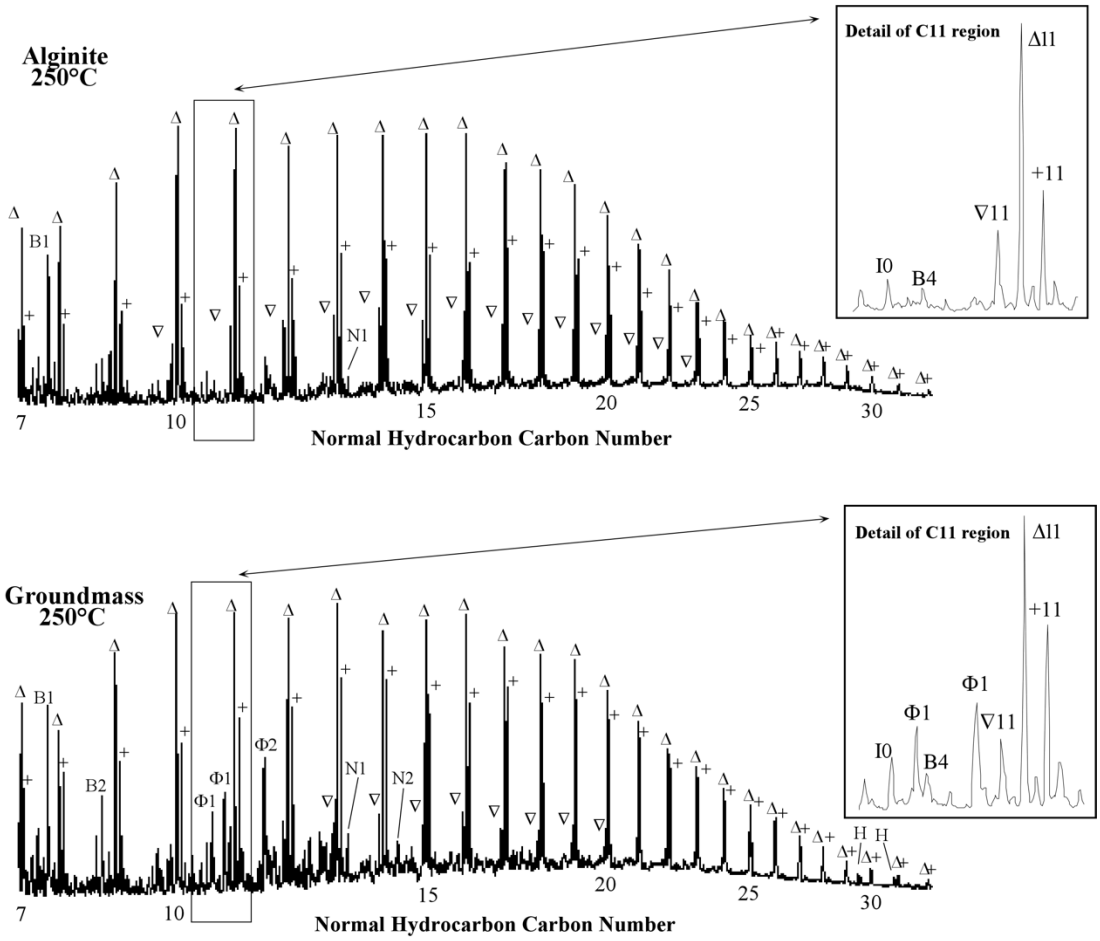

Table 2. Peak identification for pyrograms in Figures 4-6.

∇	*n*-alk-α,ω-dienes (∇11: *n*-undec-1,10-diene)
Δ	*n*-alk-1-enes (Δ11: *n*-undec-1-ene)
+	n-alkanes (+11: *n*-undecane)
B1	toluene
B2	xylenes
B4	C_4-alkylbenzenes
Φ1	cresols
Φ2	2,4- & 2,5-dimethylphenols
I0	indene
N	naphthalene
N1	1-methylnaphthalene
N2	1,3- & 1,6- & 1,7-dimethylnaphthalenes
H	hopanes and hopenes

Figure 5. Total ion current traces of the flash pyrolyzates (620°C) of the solvent-extracted residues after heating Stellarton organic groundmass and alginite at 350°C and 70 MPa for 24 hr. Insets provide details of the *n*-C_{11} region.

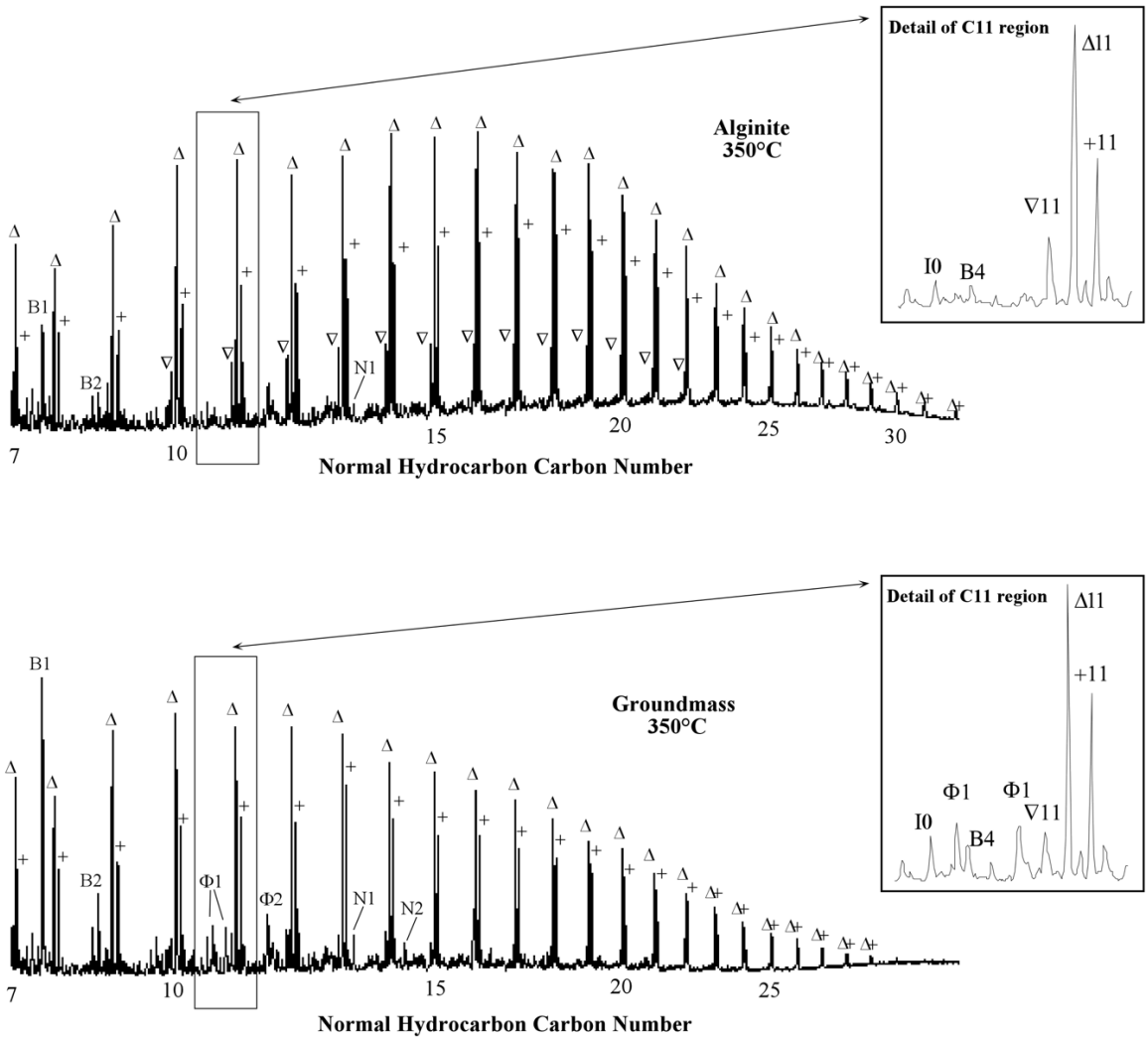

Figure 6. Total ion current traces of the flash pyrolyzates (620°C) of the solvent-extracted residues after heating Stellarton organic groundmass and alginite at 375°C and 70 MPa for 24 hr. Insets provide details of the *n*-C_{11} region.

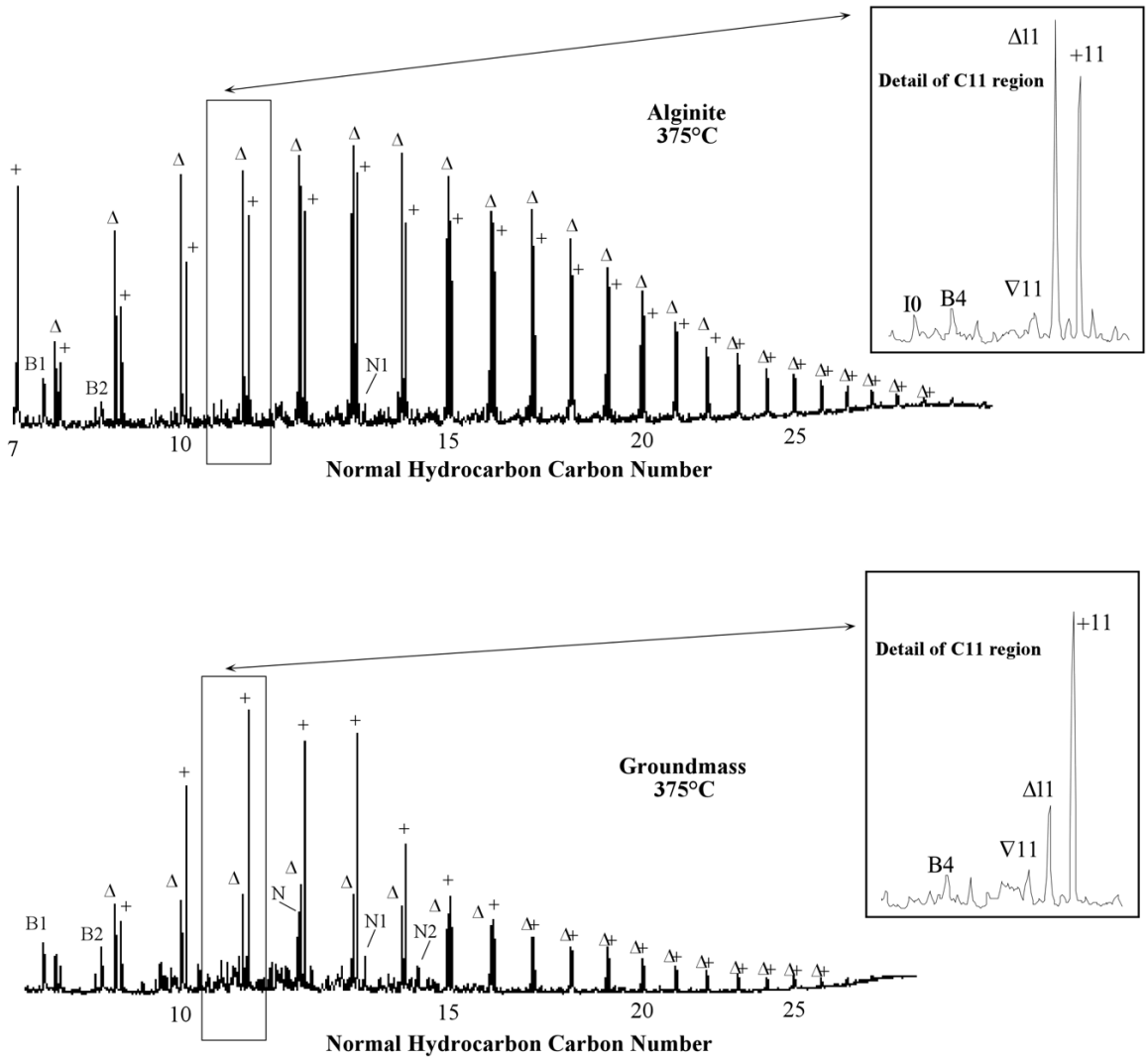

Figure 7. The trimethylnaphthalene ratio as a function of the Rock Eval hydrogen index for the extracted residues produced by confined heating of the groundmass and alginite at temperatures from 250-375°C. The trimethylnaphthalenes were quantitated using m/z 170 mass chromatograms of the flash pyrolysis-GC/MS data. The ratio is defined as the sum of 1,3,7- + 1,3,6- + 2,3,6-trimethylnaphthalenes divided by the sum of 1,4,6- + 1,3,5- + 1,2,7- + 1,6,7- + 1,2,6- + 1,3,7- + 1,3,6- + 2,3,6-trimethylnaphthalenes. There were no 325 and 375° data available for the King groundmass.

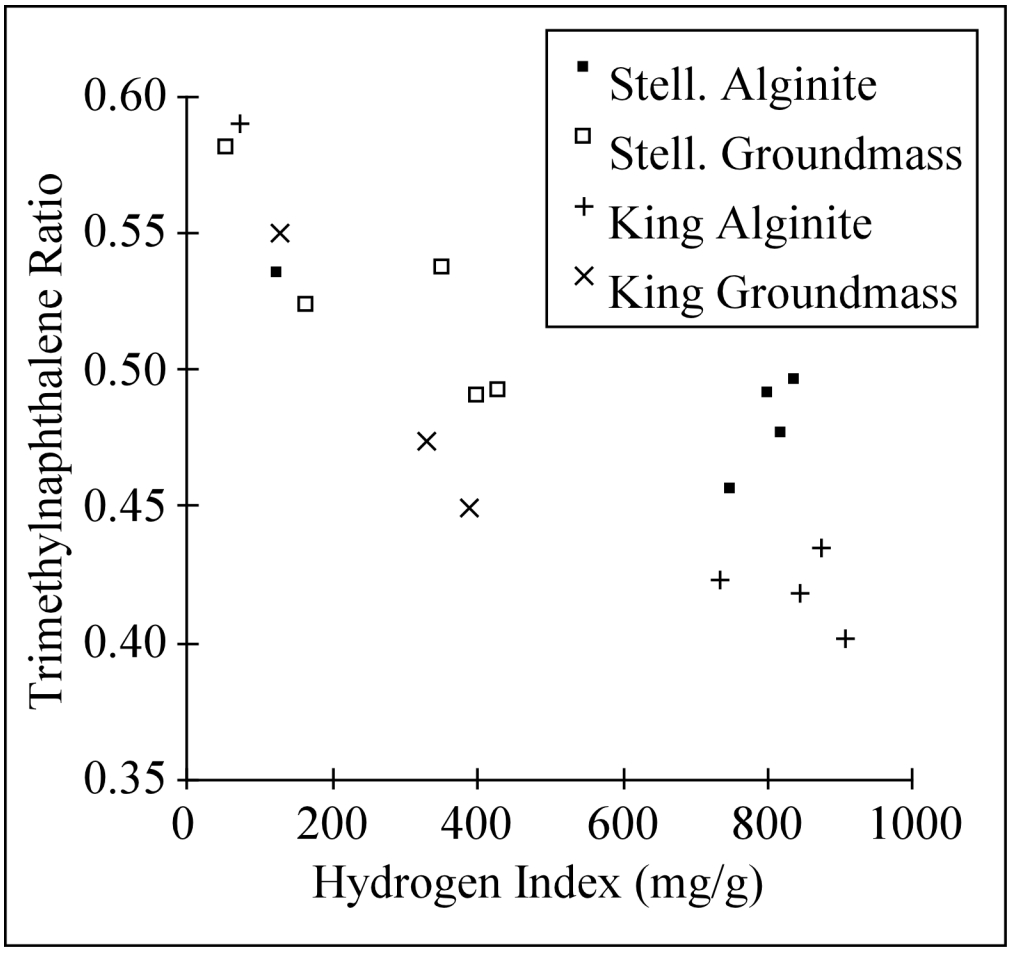

Molecular characterization of extractable organic matter

Normal alkanes were the principal compounds in the saturate fractions of the EOM generated during the heating experiments, particularly the long chain homologues, as would be expected for organic matter of lacustrine origin. While this basic observation applies in general, there were nevertheless significant variations in *n*-alkane distribution attributable to the different starting materials and temperatures employed. At 300°, the Stellarton alginite produced more *n*-alkanes in the C_{19}-C_{22} range, while the groundmass had relatively more C_{25}-C_{29} (Fig. 8). The differences apparent in the C_{15}-C_{18} range were artifacts of sample preparation. By 350°, there were no major changes in *n*-alkane distribution for the alginite, but the alkanes of the groundmass revealed a shift towards shorter chain lengths, such that the two products coincidentally appeared similar (Fig. 8). At 375°, the shift towards lower carbon numbers continued to progress for the groundmass, while such a shift began to occur for the alginite, which exhibited an increase in C_{15}-C_{22} alkanes. As seen in the results presented above, the alginite evinced little modification until the final temperature step, while the groundmass displayed a more gradual transformation, commencing at a lower temperature.

Hopanes were major constituents of the extract of the Stellarton groundmass heated at 250°. Their relative concentrations dropped precipitously with progressively higher temperatures, reaching negligible levels by 375° (Fig. 9). The extracts of the heated Stellarton alginite contained low concentrations of hopanes relative to *n*-alkanes, even after only low temperature heating. Hopanoids were also detected by Py-GC/MS in the 250° groundmass residue (Fig. 4), as was noted above. The groundmass was therefore shown to be significantly enriched in hopanoid components, indicating that prokaryotic bacteria had contributed to its formation, by altering primary organic matter (humic and algal) and/or by direct input of bacterial biomass. Classical hopane maturity parameters using the relative concentrations of moretanes or (22R) homohopane showed little significant change for the Stellarton macerals heated from 250-350°, due to the early oil window maturity of the initial sample. Hopanes were practically undetectable in the products of the 375° experiments. The hopane parameters were more useful for the King series, although they consistently indicated a higher apparent maturity for the groundmass than for the alginite heated at the same temperature. Sterane concentrations were negligibly low in both King and Stellarton series.

C_2 to C_4-alkylnaphthalenes, as well as phenanthrene, anthracene and their C_1 to C_3-alkylated derivatives were the most abundant compounds detected in the EOM aromatic fractions. The most dramatic changes in the distribution of temperature-sensitive polyaromatic hydrocarbon isomers occurred at the 375° heating step. Anthracenes were particularly important confined pyrolysis products. Since anthracenes are not significant components of petroleum, confined pyrolysis was shown to fail to fully imitate natural hydrocarbon generation. Since anthracenes are more thermally labile than phenanthrenes, monitoring the proportions of these two

types of compounds also provides a means for observing the progress of thermal alteration. The anthracenes were remarkably abundant in the EOM collected after the low temperature (250 and 300°) King alginite experiments, as exemplified by the ratio of the principal methylanthracene peak to 3- and 2-methylphenanthrenes (Fig. 10). This ratio dropped rapidly after 300°, but always remained above the value for the groundmass heated at the same temperature. Although the relative effects of progressive heating were clearly demonstrated, the OM type profoundly influenced the parameter. Since the King alginite was strongly aliphatic, initial aromatization occurring at low levels of thermal stimulation evidently also yielded "linear" products (i. e., anthracenes), by cross-linking and aromatizing adjacent alkyl chains. Anthracenes were also relatively more important in the Stellarton alginite than in the groundmass and diminished with increasing thermal alteration, but these phenomena were much less extreme than in the King series.

Figure 8. *n*-Alkane distributions in the saturate fractions of the extractable organic matter from the Stellarton alginite and groundmass heating experiments. Quantitations performed on m/z 99 mass chromatograms.

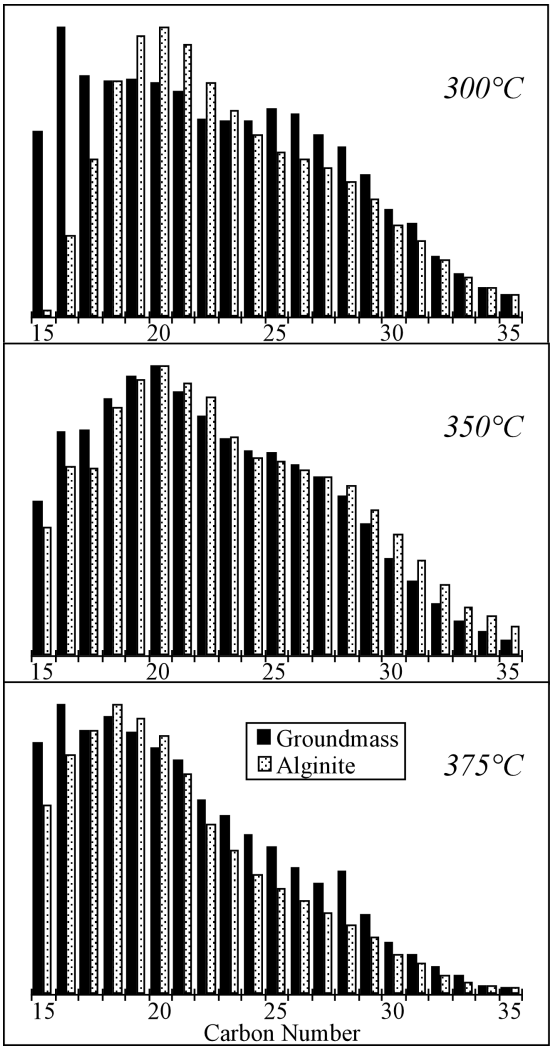

Figure 9. Hopane/*n*-alkane ratios for the Stellarton alginite and groundmass as a function of confined pyrolysis temperature. Quantitations performed on m/z 191 (hopanes) and m/z 99 (*n*-alkanes) mass chromatograms.

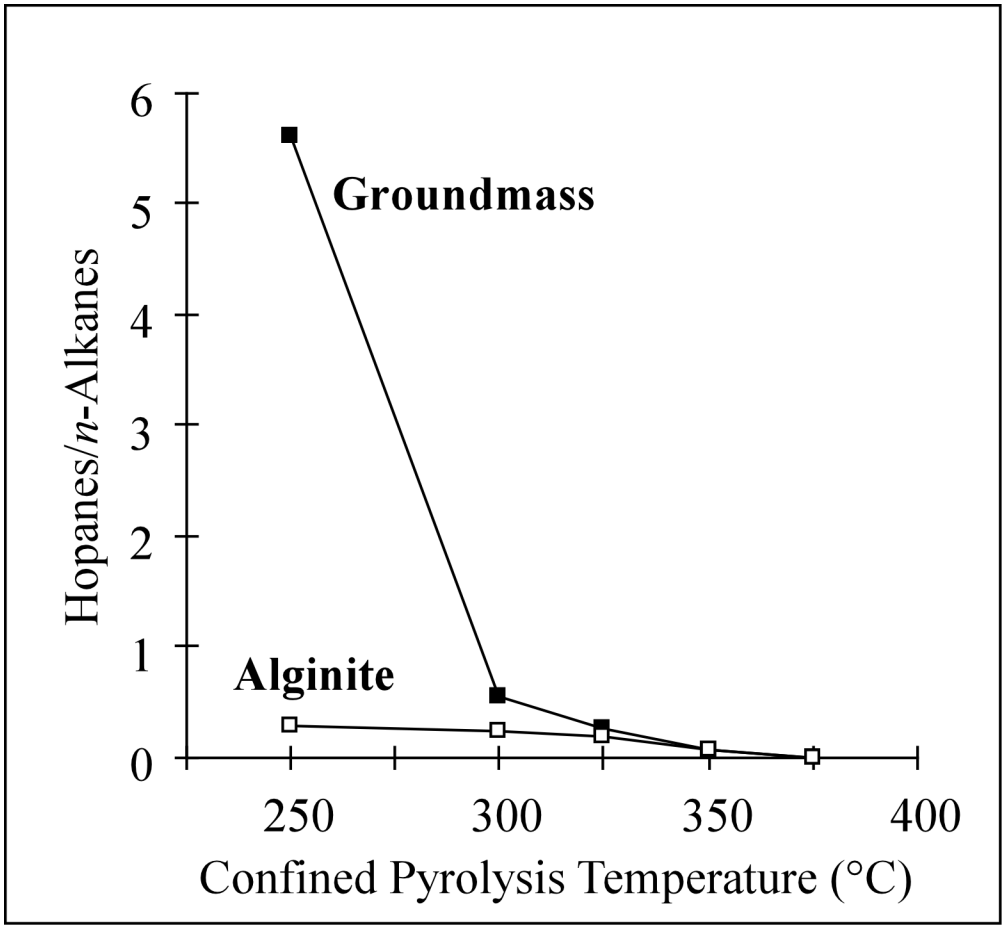

Figure 10. The methylanthracene ratio as a function of confined pyrolysis temperature for the King Cannel alginite and groundmass (EOM, aromatic fraction). Partial m/z 192 mass chromatograms of the methylanthracene (MA) and methylphenanthrene (MP) region display the results of several of the heating experiments performed on King Cannel macerals. Peak a: 3-MP, peak b: 2-MP, peak c: unspecified MA isomer, peak d: 9-MP, peak e: unspecified MA isomer and peak f: 1-MP. The definition of the ratio is also given (the MA in the ratio corresponds to peak c).

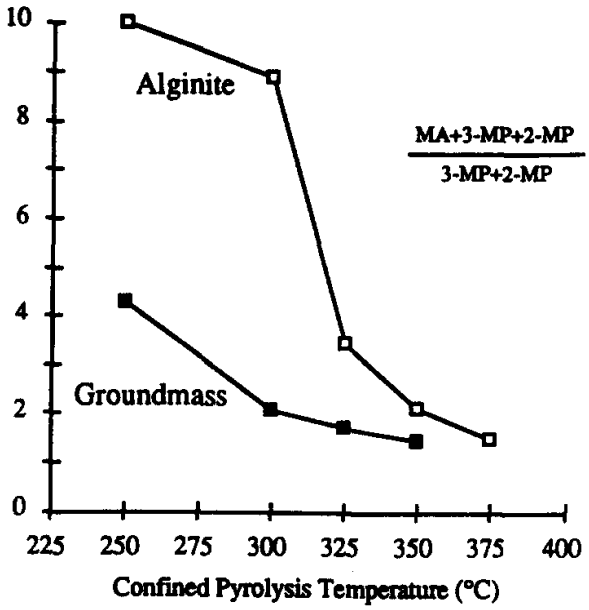

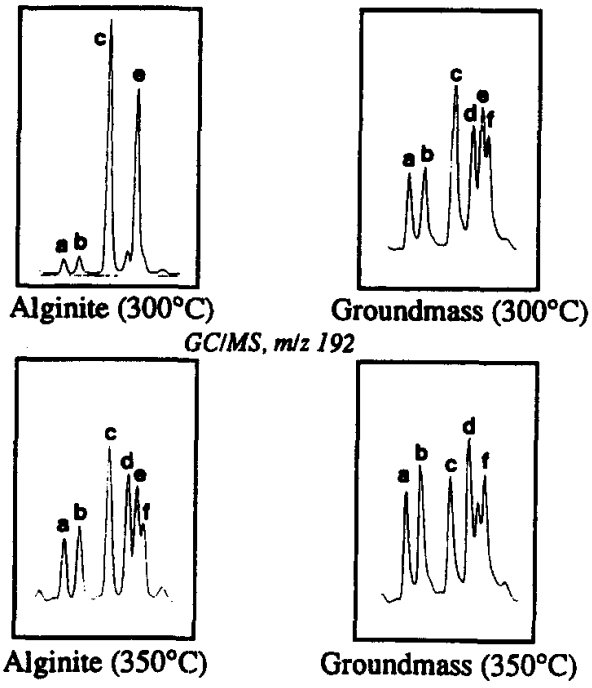

Implications for petroleum generation from torbanites

The organic groundmass and alginite separated from the same torbanite differed from each other in the amount and type of liquid products generated and in the amount of thermal stimulation necessary to do so. As documented by almost every parameter discussed, alginites derived from the resistant biopolymer of *Botryococcus* escaped thermal degradation until the highest temperature level employed in this study (375°C). At that temperature, the conversion was nearly total. In contrast to this sudden, late-stage transformation, the organic groundmass isolated from the same torbanite samples underwent a more gradual conversion as temperatures were increased, reaching peak generation at only 350°C.

Differences in the thermal responses of the alginite and groundmass can be related to their composite activation energies and ultimately to their biological precursors and early diagenetic history. The gradual thermal transformation experienced by the groundmass implies compositional heterogeneity and a broad distribution of activation energies, much like that derived for Type II kerogen by Tissot and others (1987). In contrast, the abrupt, nearly total, high-temperature conversion of the alginite indicates compositional homogeneity and a narrow range of activation energies of relatively high magnitude, much like that determined for Type I kerogen in the study just cited. The alginite flash pyrolyzates contained an overwhelming predominance of normal hydrocarbons (Figs. 4-6), clearly demonstrating the chemical homogeneity of the alginite, consistent with its origin from the aliphatic biopolymer of the thick outer cell walls of *Botryococcus*. The groundmass was shown to contain aliphatic moieties (likely derived from the less resistant portions of *Botryococcus*, from other, less resistant algae and from bacteria), phenolic moieties (from higher plant lignin) and hopanoids (from prokaryotic bacteria). The latter two components were shown to be released at lower temperatures, while normal hydrocarbons were more prominent in the higher temperature generation products. Thus the diversity of biological origin for the groundmass was reflected in the sequence of liquids generated.

In nature, petroleum generated from a torbanite would be a mixture of the liquids produced by each of its components, in a blend that would change as thermal alteration progressed, as the various constituents each reached their window of generation. The overall generation curve would be the proportional sum of the reaction progress curves for the decomposition of the individual components. Alginite, having an initial petroleum potential double that of the groundmass, would, on a gram-for-gram basis, have a greater influence on the shape of its composite curve. By varying the proportions of the two main organic components of torbanite (*Botryococcus*-related alginite and groundmass), the yield maximum would either be shifted to the "earlier" or "later" regions of the generation curve. For example, an alginite-dominated torbanite would produce more liquids — and produce them at higher levels of maturity — than would a groundmass-rich torbanite. Such a two-component model of torbanite composition can serve to improve predictions of oil generation from torbanites and related source rocks in sedimentary basins.

CONCLUSIONS

The alginite and organic groundmass fractions isolated from two torbanites displayed distinct differences in chemical and thermal properties. The alginite was rich in normal hydrocarbon moieties, consistent with its origin as the aliphatic, resistant biopolymer of the outer cell walls of *Botryococcus*. The groundmass, while still aliphatic, also contained aromatic, phenolic and hopanoid structures, reflecting mixed origins from degraded algal, bacterial and terrestrial plant debris. The 250, 300 and 325°C experiments run on alginite produced very low yields of $CHCl_3$-extractable organic matter (EOM), indicating that very little of the generation potential had been tapped. The alginite reached the onset of generation at 350° and peaked at 375°. The groundmass exhibited a distinctly different response to heating. Its 300, 325 and 350°C experiments showed a progressive increase in EOM yield with increasing temperature, producing more EOM than the corresponding alginite runs, in spite of the lower initial generation potential of the groundmass. However, EOM yields were lower at 375°C, indicating that its peak generation had occurred at 350°. Rock Eval hydrogen index data, measured on solvent-extracted residues of the heating experiments, showed essentially the same trends. Molecular maturity parameters tended to indicate a lower apparent level of maturation for the alginite EOM than for EOM of groundmass heated at the same temperature.

These findings have implications for studies of the changes in the chemical structure of kerogen as it matures, as well as for modeling oil generation processes. In nature, petroleum generated from a torbanite would be a mixture of the liquids generated by each of its components, in a blend that would change as thermal alteration progressed, as the various constituents each reached their peak of generation. The multi-component model of torbanite composition herein employed can serve to improve predictions of oil generation from torbanites and related source rocks in sedimentary basins.

Acknowledgments — The authors gratefully acknowledge financial support from CREGU and the CNRS, without which this work would not have been possible. We would also like to thank J. Crelling, A. Stankiewicz, Z. Han, C. Thies, B. Poty, S. Ashkan, M. Elie, R. Michels, L. Mansuy and all the staff at CREGU for their assistance throughout the duration of the project. We thank S. Derenne and an anonymous reviewer for their careful reading of the manuscript.

REFERENCES

Alexander R., Kagi R. I., Rowland S. J., Sheppard P. N. and Chirila T. V. (1985) The effects of thermal maturity on distributions of dimethylnaphthalenes and trimethylnaphthalenes in some ancient sediments and petroleums. *Geochim. Cosmochim. Acta* **49**, 385-395.

Bensley D. F. and Crelling J. C. (1994) The inherent heterogeneity within the vitrinite maceral group. *Fuel* **73**, 1306-1316.

Blanc P., Valisolalao J., Albrecht P., Kohut J. P., Muller J. F. and Duchene J. M. (1991) Comparative geochemical study of three maceral groups from a high volatile bituminous coal. *Energy & Fuels* **5**, 875-884.

Budzinski H., Garrigues P., Radke M., Connan J., Rayez J. C. and Rayez M. T. (1993) Use of molecular modeling as a tool to evaluate thermodynamic stability of alkylated polycyclic aromatic hydrocarbons. *Energy & Fuels* **7**, 505-511.

Combaz A. (1980) Les kérogènes vus au microscope. In *Kerogen, Insoluble Organic Matter from Sedimentary Rocks*. (Edited by Durand B.) pp. 55-111, Technip.

Comet P. A., McEvoy J., Giger W., and Douglas A.G. (1986) Hydrous and anhydrous pyrolysis of DSDP Leg 75 kerogen — a comparative study using a biological marker approach. *Org. Geochem.* **9**, 171-182.

Crelling J. C. (1988) Separation and characterization of coal macerals including pseudovitrinite. *1988 Ironmaking Conference Proceedings - AIME*, **43**, 351-356.

Crelling J. C. (1989) Separation and characterization of coal macerals: Accomplishments and future possibilities. *Am. Chem. Soc. Div. Fuel Chem. Prepr.* **34** (1), 249-255.

Derenne S., Largeau C, Casadevall E. and Connan J. (1988a) Comparison of torbanites of various origins and evolutionary stages. Bacterial contribution to their formation. Cause of the lack of botryococcane in bitumens. *Org. Geochem.* **12**, 43-59.

Derenne S., Largeau C, Casadevall E., Tegelaar E. and de Leeuw J. W. (1988b) Relationship between algal coals and resistant cell wall biopolymers of extant algae as revealed by Py-GC-MS. *Fuel Proc. Tech.* **20**, 93-101.

Dyrkacz G. R. and Horwitz E. P. (1982) Separation of coal macerals. *Fuel* **61**, 3-12.

Dyrkacz G. R., Bloomquist C. A. A. and Horwitz E. P. (1981) Laboratory scale separation of coal macerals. *Separat. Sci. Technol.* **16**, 1571-1588.

Dyrkacz G. R., Bloomquist C. A. A. and Ruscic L. (1984) High-resolution density variations of coal macerals. *Fuel* **63**, 1367-1374.

Dyrkacz G. R., Bloomquist C. A. A., Ruscic L. and Crelling J. C. (1991) An investigation of the vitrinite maceral group in microlithotypes using density gradient separation methods. *Energy Fuels* **5**, 155-163.

Given P. H., Davis A., Kuehn D., Painter P. C. and Spackman W. (1985) A multi-facetted study of a Cretaceous coal with algal affinities. I. Provenance of the coal samples and basic compositional data. *Int. J. Coal. Geol.* **5**, 247-260.

Han Z. (1995) Organic geochemistry and petrology of torbanite, cannel coal and their constituent macerals. Ph. D. thesis, Southern Illinois University at Carbondale.

Han Z., Kruge M. A., Crelling J. C. and Stankiewicz B. A. (1995) Organic geochemical characterization of the density fractions of a Permian torbanite. *Org. Geochem.* **21**, 39-50.

Hartgers W. A., Sinninghe Damsté J. S. and de Leeuw J. W. (1992) Identification of C_2-C_4 alkylated benzenes in flash pyrolyzates of kerogens, coals and asphaltenes. *J. Chromatogr.* **606**, 211-220.

Hutton A. C. (1986) Organic petrology of oil shale samples from Shaw clay pit, New Glasgow, Pictou county, Nova Scotia. Unpublished report. Nova Scotia Dept. of Mines and Energy, Halifax.

Kalkreuth W. and Macauley G. (1987) Organic petrology and geochemical evaluation (Rock Eval) studies on oil shales and coals from the Pictou and Antigonish aresa, Nova Scotia, Canada. Can. Petr. Geol. Bull. **35**, 263-295.

Kalkreuth W., Naylor R., Pratt K. and Smith W. (1990) Fluorescent properties of alginite-rich oil shales from the Stellarton Basin, Canada. *Fuel* **69**, 139-144.

Kruge M. A. and Landais P. (1992) Artificial maturation of coal and maceral concentrates: Saturate and polyaromatic molecular markers. *Amer. Chem. Soc. Div. Fuel Chem. Prepr.* **37** (4), 1595-1600.

Kruge M. A. and Bensley D. F. (1994) Flash pyrolysis-gas chromatography-mass spectrometry of Lower Kittanning vitrinites. Changes in distributions of polyaromatic hydrocarbons as a function of coal rank. In *Vitrinite Reflectance as a Maturity Parameter* (Edited by Mukhopadhyay P. K. and Dow W.) Amer. Chem. Soc. Symp. Series 570. pp. 136-148.

Kruge M. A., Crelling J. C. and Rimmer S. M. (1989) Organic geochemical and petrographic analysis of pure macerals from the Ohio Shale. *Proc. 1988 Eastern Oil Shale Symposium*, p. 411-417. Inst. for Mining and Minerals Research, Lexington, KY, USA.

Kruge M. A., Crelling J. C., Hippo E. J. and Palmer S. R. (1991) Aspects of sporinite chemistry. *Org. Geochem.* **17**, 193-204.

Landais P., Michels R., Poty B. and Monthioux M. (1989a) Pyrolysis of organic matter in cold-seal pressure autoclaves. Experimental approach and applications. *J. Appl. Anal. Pyrol.* **16**, 103-115.

Landais P., Muller J.-F., Michels R., Oudin J.-L. and Zaugg P. (1989b) Comparative behaviour of coal and maceral concentrates during artificial coalification. *Fuel* **68**, 1616-1619.

Landais P., Zaugg P., Monin J.-C., Kister J. and Muller J. F. (1991) Experimental simulation of the natural coalification of coal maceral concentrates. *Bull Soc. géol. France* **162**, 211-217.

Landais P., Rochdi A., Largeau C. and Derenne S. (1993) Chemical characterization of torbanites by transmission micro-FTIR spectroscopy - origin and extent of compositional heterogeneities. *Geochim. Cosmochim. Acta* **57**, 2529-2539.

Landais P., Michels R. and Elie M. (1994) Are time and temperature the only constraints to the simulation of organic matter maturation. *Org. Geochem*. **22**, 617-630.

Largeau C., Derenne S., Casadevall E., Kadouri A. and Metzger P. (1984) Formation of *Botryococcus*-derived kerogens. Comparative study of immature torbanite and of the extant alga *Botryococcus braunii*. *Org. Geochem*. **6**, 327-332.

Lewan, M.D. (1985) Evaluation of petroleum generation by hydrous pyrolysis experimentation. *Phil. Trans. R. Soc. Lond. A* **315**, 123-134.

Macauley G. and Ball F. D. (1984) Oil shales of the Big Marsh and Pictou areas, Nova Scotia. Open File Rep. OF1037, Inst. Sed. Petrol. Geol., Geol. Surv. Can., 57 p.

Michels R and Landais P. (1994) Artificial coalification — comparison of confined pyrolysis and hydrous pyrolysis. *Fuel* **73**, 1691-1696.

Michels R., Landais P., Torkelson B. E., and Philp R. P. (1995) Effects of effluents and water pressure on oil generation during confined pyrolysis and high-pressure hydrous pyrolysis. *Geochim. Cosmochim. Acta*. **59**, 1589-1604.

Monthioux M., Landais P. and Monin J.-C. (1985) Comparison between natural and artificial maturation series of humic coals from the Mahakam delta, Indonesia. *Org. Geochem.* **8**, 275-292.

Monthioux M., Landais P. and Durand B. (1986) Comparison between extracts from natural and artificial maturation series of Mahakam delta coals. *Org. Geochem.* **10**:299-311.

Naylor R. D. and Smith W. D. (1986) Stratigraphy, lithology and composition of the Stellarton Group oil shales, Pictou county, Nova Scotia. Nova Scotia Dept. of Mines and Energy, Open File Rep. 86-051, 114 p.

Nip M., de Leeuw J. W. and Schenck P. A. (1988) The characterization of eight maceral concentrates by means of Curie point pyrolysis-gas chromatography and Curie point pyrolysis-gas chromatography-mass spectrometry. *Geochim. Cosmochim. Acta* **52**, 637-648.

Nip M., de Leeuw J. W. and Crelling J. C. (1992) Chemical structure of bituminous coal and its constituent maceral fractions as revealed by flash pyrolysis. *Energy & Fuels* **6**, 125-136.

Püttman W. and Kalkreuth W. (1989) Comparison of hydrocarbon compositions in a sequence of humic coals and oil shales from the Pictou Colfield, Nova Scotia. *Atlantic Geol.* **25**, 93-103.

Radke M., Garrigues P. and Willsch H. (1990) Methylated dicyclic and tricyclic aromatic hydrocarbons in crude oils from the Handil field, Indonesia. *Org. Geochem.* **15**, 17-34.

Requejo A. G., Gray N. R., Freund H., Thomann H., Melchior M. T., Gebhard L. A., Bernardo M., Pictroski C. F. and Hsu C. S. (1992) Maturation of petroleum source rocks. I. Changes in kerogen structure and composition associated with hydrocarbon generation. *Energy & Fuels* **6**, 203-214.

Saxby J. D., Bennett A. J. R., Corcoran J. F., Lambert D. E., and Riley K. W. (1986) Petroleum generation: Simulation over six years of hydrocarbon formation from torbanite and brown coal in a subsiding basin. *Org. Geochem.* **9**, 69-81.

Senftle J. T., Yordy K. L., Barron L. S. and Crelling J. C. (1988) Analysis of mixed kerogens from Upper Devonian New Albany Shale I. Evaluation of kerogen

components derived from density separation. *Proc. 1987 Eastern Oil Shale Symposium.* Kentucky Energy Cabinet, Lexington, Kentucky, p. 155-167.

Sinninghe Damsté J. S., de las Heras F. X. C. and de Leeuw J. W. (1992) Molecular analysis of sulfur-rich brown coals by flash pyrolysis-gas chromatography-mass spectrometry. *J. Chromatogr.* **607**, 361-376.

Sinninghe Damsté J. S., de las Heras F. X. C., van Bergen P. F. and de Leeuw J. W. (1993) Characterization of Tertiary Catalan lacustrine oil shales: Discovery of extremely organic sulfur-rich Type I kerogens. *Geochim. Cosmochim. Acta* **57**, 389-415.

Smith W. D., St. Peter C. J., Naylor R. D., Mukhopadhyay P. K., Kalkreuth W., Ball F. D. and Macauley G. (1991) Composition and depositional environment of major eastern Canadian oil shales. *Int. J. Coal. Geol.* **19**, 385-438.

Stankiewicz B. A. (1995) Geochemistry and petrology of coal and kerogen macerals. Ph. D. thesis, Southern Illinois University at Carbondale.

Stankiewicz B. A., Kruge M. A. and Crelling J. C. (1994a) Geochemical characterization of maceral concentrates from Herrin No. 6 coal (Illinois Basin) and Lower Toarcian Shale kerogen (Paris Basin). *Bull. Centres Rech. Explor.-Prod. Elf-Aquitaine* **18**, 237-251.

Stankiewicz B. A., Kruge M. A., Crelling J. C. and Salmon G. L. (1994b) Density gradient centrifugation: Application to the separation of macerals of Type I, II, and III sedimentary organic matter. *Energy & Fuels* **8**, 1523-1521.

Stout S. A. (1993) Lasers in organic petrology and organic geochemistry, II. In situ laser micropyrolysis-GCMS of coal macerals. *Int. J. Coal Geol.* **24**, 309-331.

Tannenbaum E., Ruth E., and Kaplan I.R. (1986) Steranes and triterpanes generated from kerogen pyrolysis in the absence and presence of minerals. *Geochim. Cosmochim. Acta* **50**, 805-812.

Tissot B. P., Pelet R. and Ungerer Ph. (1987) Thermal history of sedimentary basins, maturation indices and kinetics of oil and gas generation. *AAPG Bull.* **71**, 1445-1466.

Yawanarajah S. R. and Kruge M. A. (1994) Lacustrine shales and oil shales from Stellarton Basin, Nova Scotia, Canada: organofacies variations and use of polyaromatic hydrocarbons as maturity indicators. *Org. Geochem.* **21**, 153-170.